

EFFECT OF OXIDATION OF SiC ON AGING CHARACTERISTICS OF SiC PARTICLES AND SHORT MULLITE FIBERS REINFORCED 2024Al COMPOSITE^①

Mei Zhi

*Department of Materials, Huazhong University of Science
and Technology, Wuhan 430074, P. R. China*

Jin Yanping, Gu Mingyuan and Wu Renjie
*State Key Laboratory of Metal Matrix Composites,
Shanghai Jiao Tong University, Shanghai 200030, P. R. China*

ABSTRACT The effect of oxidation of SiC particles on the aging behavior of SiC particles and short mullite fibers reinforced 2024Al composite was investigated. Differential scanning calorimetry (DSC) analysis indicated that the aging precipitation in specimen with as-received SiC particles lagged behind that of unreinforced 2024Al, while in specimen with oxidized SiC particles the precipitation of the GP zone slightly lagged behind that of unreinforced 2024Al, but the precipitation of the S' phase was accelerated and a new peak appeared after the S' peak. On the basis of the results of DSC analysis and TEM observation, it was believed that all these facts were resulted from the interactions among SiC (as-received or oxidized) particles, mullite fibers and the matrix.

Key words aluminum matrix composite SiC mullite fiber 2024Al alloy aging

1 INTRODUCTION

Aging treatment has been widely used as a further strengthening means for aluminum matrix composites. Study of composites' aging law and mechanism not only helps to draw up optimum aging technology parameters, but also provides important theory basis and experimental data. Several papers have reported the aging characteristics of silicon carbide particulates reinforced 2024Al composite^[1-3], but the research of effect of silicon carbide particles' oxidation on aging behavior of the composites has rarely been reported. In this paper, the effect of silicon carbide's surface oxidation on aging behaviors of silicon carbide particles and mullite fibers reinforced 2024Al composites was investigated.

2 EXPERIMENTAL

The green and abrasive grade α -SiC particles with an average size of $60 \mu\text{m}$ were used in the present work. Artificial oxidation of the particle was carried out in air at 1100°C for 10h using an Al_2O_3 crucible heated in an electric furnace. In order to guarantee the uniform distribution of SiC particles among 2024Al matrix, 15% (volume fraction) short fiber of mullite (containing 72% Al_2O_3 and 28% SiO_2) and 15% (volume fraction) particulates of SiC were used as reinforcements. The composite samples were squeeze cast from a melt of commercially 2024Al alloy whose composition was shown in Table 1. Other details of sample preparation were described elsewhere^[4]. The SiC particles added

^① Project 59291000 supported by the National Natural Science Foundation of China and project supported by the State Key Laboratory of Metal Matrix Composites in Shanghai Jiao Tong University

Received Sep. 10, 1997; accepted May 26, 1998

were either as received or artificially oxidized for the sake of comparison. Corresponding composite materials are designated as composite-A and composite-O respectively.

The specimens for differential scanning calorimetry (DSC) analysis were solutionized at 500 °C for 1.5 h followed by quenching in ice-brine. In case of aging, then they were kept in refrigerator before testing. DSC measurements were performed using a Perkin Elmer DSC-7 apparatus. Runs were carried out at a heating rate of 20 °C/min from 20 to 450 °C and under a dynamic dry nitrogen atmosphere. High purity aluminum was used as a reference. DSC thermograms were normalized to one gram weight of testing material.

Table 1 Composition of 2024 alloy (in mass, %)

Cu	Mg	Mn	Al
3.8~4.9	1.2~1.8	0.3~0.9	Balance

Microstructural and compositional examinations were carried out in a Philips CM-12 electron microscope at 100 kV. Samples for transmission electron microscopy (TEM) were prepared by standard methods involving mechanical grinding, polishing and dimpling followed by ion milling of foil to perforation.

3 RESULTS

Fig. 1 is DSC thermograms of composite-A and composite-O. For comparison purposes, the thermogram of 2024Al is also shown in the figure. The curve from 2024Al in Fig. 1 shows four zones: exothermic between 40 °C and 135 °C due to the formation of GP zones, endothermic between 135 °C and 260 °C due to the dissolution of GP zones, exothermic between 260 °C and 320 °C due to the formation of S' precipitate, and endothermic between 320 °C and 450 °C due to the dissolution of S' precipitate. This result is similar to those reported in Ref. [1]. The overall characteristics of the composite-A and composite-O are not changed, but some aspects of the reaction are altered.

It can be seen that the addition of SiC reinforcements did not change the sequence of the precipitation reactions in aluminum matrix, the same precipitation and dissolution reaction occurred in the composites as in the unreinforced 2024 alloy, but the kinetics of the GP zone and the S' phase formation and dissolution reaction were changed in the composites. In composite-A, as the kinetics of the GP zone and the S' phase formation and dissolution reactions were decelerated, so its corresponding DSC curve was shifted towards high temperature. While in composite-O, the exothermic peak corresponding to GP formation was slightly suppressed, but the exothermic peak corresponding to S' formation was accelerated, and a new peak appeared after the S' peak.

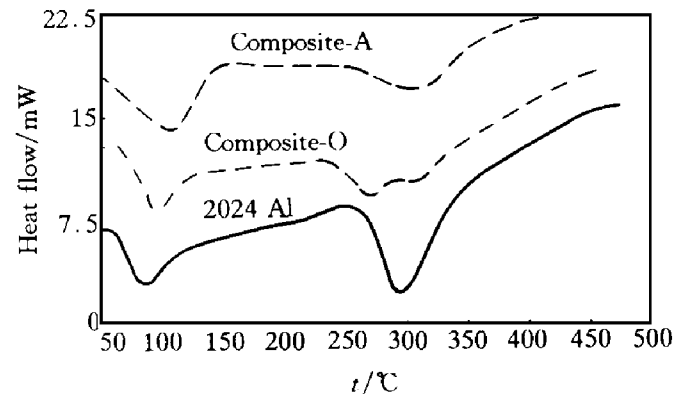


Fig. 1 DSC curves of unreinforced 2024Al, composite-A and composite-O

On the other hand, the addition of SiC particles and mullite fibers also reduced the enthalpies of GP zone formation and S' phase precipitation. According to the theory of thermal analysis^[5], the peak area on thermal curve in Fig. 1 corresponds to enthalpy change caused by corresponding reaction, and the relation between reaction enthalpy (or reaction heat) and volume fraction (V_f) of reaction product is as follows:

$$\Delta H = \frac{\Delta H_p}{M_p} \times \frac{\rho_p}{\rho_s} V_f \quad (1)$$

where ΔH_p represents reaction heat per mole, M_p represents relative molecular mass of the precipitate, ρ_p and ρ_s represent densities of the precipitate and the sample, respectively.

From the above equation, the change of reaction entropy is directly proportional to the volume fraction of reaction product. Table 2 shows the enthalpies and temperatures for the formation of GP zone and S' phase.

Table 2 Enthalpies and temperatures for the formation of GP zone and S' phase

Materials	GP Zone		S' Phase	
	ΔH (J \cdot g $^{-1}$)	T_p / °C	ΔH (J \cdot g $^{-1}$)	T_p / °C
2024Al	9.2	83	28.8	294
Composite A	8.3	108	6.9	311
Composite O	7.5	93	4.2	272

4 DISCUSSION

As for the effect of silicon carbide addition on the aging precipitation in 2024Al, it has been reported that the aging precipitation of composites (including S' and θ) was accelerated by the addition of silicon carbide. Nevertheless, when examining the changing causes of DSC curves for composite reinforced by silicon carbide particulates and mullite fibers, it is believed that the effect of both silicon carbide particulates and mullite fibers should be considered.

4. 1 Lagging cause of composite A's DSC curve

According to Lin's results^[1], when as-received silicon carbide was solely used as reinforcement, compared with unreinforced 2024Al alloy, the precipitation of both GP zone and S' phase was accelerated, and their corresponding reaction enthalpies were obviously reduced, but the overall characteristics of the composite was not changed.

When using only as-received silicon carbide as reinforcement, on one hand, interfaces in the material are increased largely; on the other hand, due to the large difference of thermal coefficients between ceramics reinforcement and aluminum (1: 10). When being cooled from high temperature, high densities of dislocation are produced in the matrix. The increased densities of dislocation result in increased diffusion speed

of alloy element. So the precipitation temperatures of GP zone and S' phase are lowered, and DSC curve shifts to lower temperatures. At the same time, because the dislocation and interface become the sunk of retained vacancies, the number of GP zones formed is reduced. Meanwhile as alloy element segregates to the interface between SiC and Al or precipitates formed alone the interface, the poorness of alloy element in adjacent of interface and interior matrix is caused, the formation of intermediate S' phase is suppressed or reduced. As a result, the enthalpies of GP zone and S' phase are obviously reduced.

Nevertheless, after using as-received silicon carbide and mullite fiber as reinforcement, on one hand, the factors of silicon carbide causing GP zone and S' phase accelerative precipitation still exist; on the other hand, the effects of short mullite fiber could not be ignored.

After being added to 2024Al matrix, the short mullite fibers have a strong affinity to alloy element Mg because it contains some amount of SiO_2 on the surface. Since the formation of hardening precipitation requires a critical ratio of the active alloy elements (i. e. Cu/Mg), such compositional variations should significantly alter the age-hardening response of matrix alloys. This is called chemical effect. On the other hand, large amounts of introduced fiber/matrix interface become the sunk of retained quenched-in vacancies, so large amounts of vacancies disappear on these interfaces. According to Ref. [6], vacancies play a key role in the formation of GP zone, because they provide nucleating sites for the formation of GP zone in all kinds of form. So the precipitation of GP zone is lagged behind. That is the so-called physical effect. Due to the combination of chemical and physical interactions, therefore the available evidence suggests that the age-precipitating is strongly impaired by short mullite fibers, which was reflected in the results of Friend^[7] and Chen^[8].

TEM analysis shows that the S' phases precipitating on the interface between mullite and matrix (Fig. 2(a)) is far coarser than that on the interface between SiC and matrix in composite A (Fig. 2(c)). It indicates that the suppression of

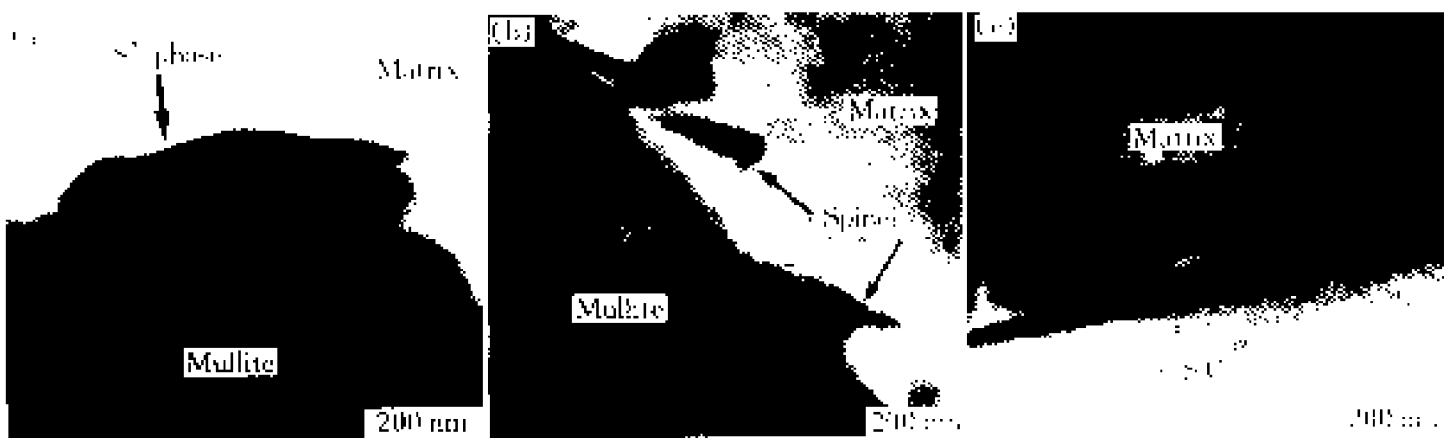


Fig. 2 Microstructures of composite A

(a) —Large S' phase precipitated in mullite/ matrix interface;
 (b) —Some spinel formed in mullite/ matrix interface; (c) —Morphology of SiC_p/ matrix interface

mullite fiber to age-hardening exceeds the acceleration of as-received SiC to age-precipitating, therefore the entire composite A behaves as lagging. And as the short mullite fiber contains some amount of SiO₂ on its surface, some spinel (MgAl₂O₄) is formed on mullite/matrix interface.

4.2 Explanation of composite O's DSC curve

According to our previous research^[9], an oxidation layer (namely, SiO₂) of about 500 nm will be formed on the surface of silicon carbide after oxidation. During the initial processing and fabrication of the composite, the oxidation layer reacted with the magnesium in matrix to form a

bandy reaction product, MgAl₂O₄ (Fig. 3(c)), while only a small amount of tiny S' phase precipitated on the interface between short mullite fiber and matrix (Fig. 3(a)), and no spinel was formed on mullite/matrix interface (Fig. 3(b)). These indicated that the affinity of oxidation on silicon carbide's surface for magnesium exceeds the affinity of short mullite fiber for magnesium. As a result, the magnesium needed for aging precipitation are largely attracted to the surroundings of oxidized silicon carbide, and the chemical effect of short mullite fibers is greatly reduced. Therefore, in comparison with as-received silicon carbide, the effect of silicon carbide on aging precipitation is largely accelerated.

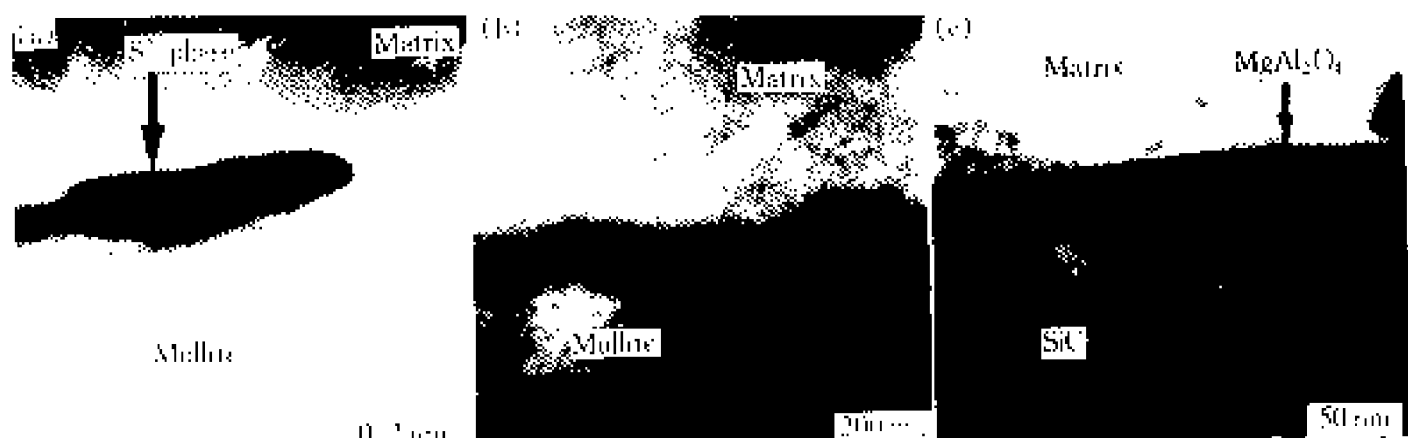


Fig. 3 Microstructures of composite O

(a) —Small S' phase precipitated in mullite/ matrix interface;
 (b) —No spinel formed in mullite/ matrix interface; (b) —SiC_p/ matrix interface

Meanwhile, short mullite fiber's physical effect on aging precipitation still exists. So the precipitation of GP zone remains suppressed, but the extent of suppressing is reduced, which is reflected from the precipitating temperature of GP zone.

As for the dual-peak phenomenon of composite-O, it is related to the reaction occurred after addition of oxidized silicon carbide to 2024Al matrix. The reaction formula can be expressed as



It means that there exists a precipitation of silicon phase in the matrix, except for the formation of MgAl_2O_4 on the surface of oxidized silicon carbide. In the course of DSC scanning, the silicon phase which is dissolved into matrix after sample's solution treatment precipitates once again near the temperature of 300 °C, resulting in the appearance of corresponding exothermic peak in DSC curve. Similar phenomenon was also reported in Ref. [10]. As for the reason for no dual-peak phenomenon in the DSC curve of composite-A, probably it is due to the fact that the silicon content formed in the reaction between mullite fiber and magnesium in matrix is too small.

5 CONCLUSIONS

(1) The addition of reinforcements did not change the precipitation sequence of 2024 alloy in both composite-A and composite-O, but the volume fractions of GP zone and S' phase were reduced.

(2) The aging precipitation process in com-

posite-A lagged behind that in 2024Al; while in composite-O, the precipitation of GP zone slightly lagged behind that in 2024Al, but the precipitation of S' phase was accelerated, and a new peak appeared after S' peak. It was believed that these results were due to the interactions among matrix, silicon carbide particles and mullite fibers.

REFERENCES

- 1 Lin Junshan, Li Pengxing and Wu Renjie. *Acta Metallurgica Sinica*, 1992, 28(10): B465.
- 2 Chawla K K, ESmaeili A H, Datye A K *et al.* *Scripta Metallurgica et Materialia*, 1991, 25: 1315–1319.
- 3 Dyos K L, Shollock B A and Flower H M. In: Whistler B C ed, *Proceedings of ICCM-10*. Canada, 1995: 441–448.
- 4 Mei Zhi, Gu Mingyuan, Jiang Weiji *et al.* *Journal of Shanghai Jiao Tong University*, (in Chinese), 1996, 30(Sup): 116–121.
- 5 Chen Jinhong and Li Chuanry. *Thermal analysis and its application*, (in Chinese). Beijing: Science Press, 1985.
- 6 Porter D A and Easterling K E. *Phase Transformation in Metals and Alloy*. Oxford: Alden Press, 1981: 303.
- 7 Friend C M, Horsfall I, Luxton S D *et al.* In: Fishman S G and Dhingra A K eds, *Advances in Cast Metal Matrix Composites*. Metals Park, OH: ASM INTERNATIONAL, 1988: 309–15.
- 8 Chen Kuochan and Chao Chuenguang. *Metallurgical and Materials Transactions A*, 1995, 26A: 1035–1043.
- 9 Mei Zhi, Gu Mingyuan and Wu Renjie. *Acta Metallurgica Sinica*, (in Chinese), 1997, 33(5): 557.
- 10 Garcia Cordovilla C, Louis E, Narciso J *et al.* *Materials Science and Engineering*, 1994, A189: 219–227.

(Edited by Yuan Saiqian)